

Characterization and reduction of magnetic noise due to saturation in induction machines

J. Le Besnerais, *Student Member, IEEE*, V. Lanfranchi, M. Hecquet, *Member, IEEE*, G. Lemaire, E. Augis, and P. Brochet, *Member, IEEE*

Abstract— This paper derives the analytical characterization of Maxwell radial vibrations due to saturation effects in induction machines, and especially in traction motors. The number of nodes and the velocity of these particular force waves are experimentally validated by visualizing some operational deflection shapes of the stator. It is shown that according to the stator and rotor slot numbers, and stator natural frequencies, these forces can be responsible for high magnetic noise levels during electrical starting and braking. A simple rule to avoid saturation magnetic noise is then proposed, and applied to an industrial motor.

A fully analytical model of the motor vibro-acoustic behavior, including saturation effects, is finally presented. Simulation results show that the new proposed motor improves magnetic noise level up to 20 dB, whereas experiments give a 15 dB improvement.

Index Terms— Induction machine, saturation, magnetic noise, vibrations, Maxwell forces.

NOMENCLATURE

b_r	Rotor slot opening width
b_s	Stator slot opening width
d_f^r	Rotor fictitious slot depth
d_f^s	Stator fictitious slot depth
f_2	Stator mode number 2 natural frequency
f_c	PWM switching frequency
f_s	Stator current fundamental frequency
f_{mm}^s	Stator magnetomotive force (mmf)
F_0	Stator mmf magnitude
g	Air-gap width
k_a	Integers involved in saturation permeance Fourier series
K_c	Carter coefficient
k_r, k_s	Integers involved in slotting permeance Fourier series
K_s	Saturation factor
p	Number of pole pairs
P_a	Saturation permeance harmonics
P_r, P_s	Rotor and stator slotting permeance harmonics magnitude

Manuscript received the 30th of October, 2008. This work was supported in part by the French Agence De l'Environnement et de la Maîtrise de l'Energie.

J. Le Besnerais is with ALSTOM Transport, and with the Laboratoire d'Electrotechnique et d'Electronique de Puissance (L2EP), Ecole Centrale de Lille, FRANCE (e-mail: jean.le.besnerais@centraliens.net).

G. Lemaire and E. Augis are with the company VIBRATEC, Ecully, FRANCE.

V. Lanfranchi is with the LEC (Laboratoire d'Electromécanique de Compiègne), UTC, Compiègne, FRANCE (e-mail: vincent.lanfranchi@utc.fr).

M. Hecquet and P. Brochet are also with the L2EP (e-mail: michel.hecquet@ec-lille.fr and pascal.brochet@ec-lille.fr).

s	Fundamental slip
Z_r	Number of rotor slots
Z_s	Number of stator slots
α_s	Angular position in stator steady frame
μ_0	Air-gap magnetic permeability
τ_r	Rotor slot pitch
τ_s	Stator slot pitch

I. INTRODUCTION

Acoustic comfort becomes increasingly important in subway and light-rail vehicles for both passengers who can be placed close to the engine, but also for frontage residents and passers-by. As progress is being made in mechanical and aerodynamic noise reduction, the full understanding of magnetic noise generation becomes crucial. This particular source of noise, whose tonalities are penalized by IEC 60034-9 norm, is mainly due to the air-gap radial Maxwell forces which excite the stator in the audible range. Saturation effects modify the Maxwell forces spectrum, especially in starting phase where the air-gap flux is maximal in order to develop maximal torque, and can therefore create new harmful resonances.

This effect of saturation is generally not included when modelling magnetic noise [1], [2], [3], [4]. In [5], this effect is modelled but no experimental nor numerical validation is given, and the choice of slot numbers combination in order to avoid resonances due to saturation is not treated.

This paper first presents the analytical characterization of Maxwell vibrations due to saturation effects, on the ground of a fully analytical vibro-acoustic model of the induction machine called DIVA. Their characteristics (velocity, number of nodes) are experimentally validated by visualizing the stator stack deflections at some given frequencies. An experimental law of the noise level increase with saturation is also established.

A simple design rule on rotor and stator slot combination in order to avoid strong resonances due to saturation is then proposed, and applied to a given motor where saturation forces create strong vibrations. Some DIVA simulations are finally run to compare the noise radiated by the tested motor and the new proposed motor, and successfully compared to experimental results.

II. CHARACTERIZATION OF MAGNETIC NOISE DUE TO SATURATION

A. Expression of radial Maxwell forces

Magnetic forces can come from magnetostriction and Maxwell forces. Magnetostriction rather affects frequencies in-

ferior to 500 Hz [6], [7], it is assumed not to be responsible for high pitch magnetic noise. Neglecting these magnetostrictive effects, and the tangential component of Maxwell tensor, the radial exciting pressure P_M which is supposed to be the only magnetic noise source can be approximated by [8], [9], [10]

$$P_M = B_g^2 / (2\mu_0) \quad (1)$$

where B_g is the radial air-gap flux density. Assuming that the rotor is not skewed, and neglecting end-effects, this force is independent of the axial direction and can therefore only excite some circumferential modes of the stator stack, which can be modeled by an equivalent ring as a first approximation [9], [11]. Developing the magnetic pressure (1) in two-dimensional Fourier series, it can be expressed as a sum of progressive force waves of frequency f and space frequency m (spatial order) :

$$P_M(t, \alpha_s) = \sum_{m,f} A_{mf} \cos(2\pi ft - m\alpha_s + \phi_{mf}) \quad (2)$$

A magnetic noise resonance occurs at two conditions [12]: the order m of the force harmonic must be the same as the circumferential mode number of the stator (e.g. $m = 2$ for the elliptical mode), and the frequency of the force harmonic must be the same as the frequency of the natural frequency of the stator mode under consideration. In variable-speed motors, this frequency match condition is more easily satisfied as the frequencies of magnetic forces due to fundamental current vary proportionally to the supply frequency f_s , and therefore sweep a wide frequency range during starting and braking. There exist an infinite number of force harmonics, but the magnitude of the vibration waves that they generate are inversely proportional to m^4 [10], so that only the lowest spatial orders forces lead to significant vibration and noise (0 to 4 for traction motors).

In order to predict magnetic noise resonances, one must therefore analytically calculate the Fourier development of P_M . This requires an analytical model of the air-gap radial flux density distribution, for instance a permeance / magnetomotive force (mmf) decomposition [13]. In no-load case, this decomposition can be written as [14]

$$B_g = \Lambda f_{mm}^s = \frac{\mu_0}{g_f} f_{mm}^s \quad (3)$$

where g_f is the air-gap "fictitious width", i.e. the mean length of flux density lines along the air-gap, which can equal g , $g + d_f^s$, $g + d_f^r$ or $g + d_f^s + d_f^r$ according to the respective position of stator and rotor slots. The Fourier series expressions of both permeance and mmf distributions can be found in [15], [16], as well as the flux density spectrum resulting from their multiplication, and the Maxwell force spectrum obtained from the combination of flux density harmonics.

Schematically, any Maxwell pressure harmonic P_h can be written in no-load sinusoidal case as

$$P_h = \Lambda_h \Lambda_{h'} F_h F_{h'} / (2\mu_0) \quad (4)$$

where Λ_h and $\Lambda_{h'}$ are permeance fundamental or harmonics which can come either from stator slotting (Λ_s), rotor slotting (Λ_r) or their interaction (Λ_{sr}), F_h and $F_{h'}$ are stator mmf fundamental (F_0) or harmonics (F_w) which come from the discretized distribution of stator winding in slots.

B. Saturation force waves

All these combinations give numerous pressure waves. However, the higher their spatial order m is, the lower the associated stator deflection is [9]. Moreover, some of them have very low magnitude as they come from the multiplication of low magnitude harmonics (e.g. a high order mmf space harmonic combined with a high order permeance harmonics gives a very low flux density harmonic). Finally, many of these harmonics have frequencies of the form $2f_s$ and orders 0 or $2p$: they have therefore relatively low frequencies (inferior to 400 Hz), far from human's ear maximal sensitivity range ; besides, they cannot resonate with stator 0 or $2p$ modes which are near 3000 Hz in traction applications, so they are generally covered by mechanical noise.

Neglecting these force waves, one can find that they can be reduced to three main families assuming that currents are sinusoidal [17], [18]:

- 1) slotting force harmonics, coming from the interaction of some rotor and stator slotting permeance harmonics with twice the stator mmf fundamental (magnitude $\Lambda_s \Lambda_r F_0 F_0 / (2\mu_0)$)
- 2) "winding force" harmonics, coming from the interaction of some rotor and stator slotting permeance harmonics with the stator mmf fundamental, and with one stator mmf space harmonic (magnitude $\Lambda_s \Lambda_r F_0 F_w / (2\mu_0)$)
- 3) saturation force harmonics, coming from the interaction of a slotting permeance harmonics with a saturation permeance harmonic, and with twice stator mmf fundamental (magnitude $\Lambda_{sr} \Lambda_a F_0 F_0 / (2\mu_0)$)

Saturation of teeth indeed flattens the air-gap flux density, which modifies the space harmonic content of Maxwell forces, and can change magnetic noise level [9]. This effect can be modelled by adding to the permeance function additional permeance harmonics due to saturation with spatial order $2pk_a$ where k_a is a positive integer [13], [19], [20], [21]:

$$\Lambda_{sat}(t, \alpha_s) = \Lambda(t, \alpha_s) + \sum_{k_a=1}^{\infty} \Lambda_{k_a} \cos(2k_a \omega_s t + 2pk_a \alpha_s + \phi_a) \quad (5)$$

where the permeance harmonics magnitude Λ_{k_a} depend on the saturation factor and are inversely proportional to k_a . For $k_a = 1$, we have for instance [19]

$$\Lambda_1 = \frac{\mu_0}{g K_c K_s} \frac{2A_{sat}}{1 + A_{sat}} \quad A_{sat} = \frac{F_{st} + F_{rt}}{F_g + F_{sy} + F_{ry}} \quad (6)$$

where F_{st} and F_{rt} are the ampere-turns in stator and rotor teeth path, F_{sy} and F_{ry} are the ampere-turns in stator and rotor yoke paths, and F_g are the ampere-turns coming from the air-gap path.

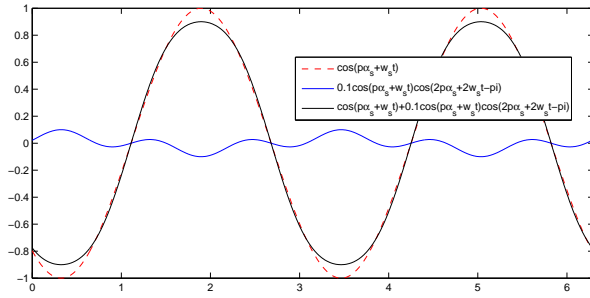


Fig. 1. Illustration of the air-gap radial flux density flattening due to even order saturation permeance waves.

The air-gap flux density distribution flattening with saturation is illustrated in Fig. 1 for $k_a = 1$.

To obtain the analytical expression of these particular force waves, one can develop all the involved quantities (permeance and mmf) in Fourier series. As saturation waves are linked to the stator mmf fundamental, the permeance harmonics expression are only needed. One can show that [22]

$$\Lambda_{sr} = \frac{1}{2} K_{sr} (\cos((k_s Z_s - k_r Z_r) \alpha_s + k_r Z_r \alpha_r) + \cos((k_s Z_s + k_r Z_r) \alpha_s - k_r Z_r \alpha_r)) \quad (7)$$

where $\alpha_r = \frac{2\pi f_s}{p} (1-s)t$ stands for a rotor bar angular position, k_r and k_s are strictly positive integers coming from the Fourier development of permeance distribution, and K_{sr} is a multiplicative coefficient proportional to $1/(k_s k_r)$.

Provided that the fundamental stator mmf is given by $F_0 \cos(p\alpha_s - 2\pi f_s t)$, one can easily find the expression of saturation force waves [18]. The obtained force harmonics are characterized in Table I where strictly positive integers k_a come from the Fourier development of saturated permeance distribution, and size the magnitude of permeance harmonics: the highest magnitude force waves are linked to $k_a = 1$, and $k_s = k_r = 1$. Note that F_{sat}^0 saturation vibrations frequencies are the same as some slotting vibrations [9], [23].

TABLE I
MAIN SATURATION FORCE LINES EXPRESSION.

Name	Frequency f	Spatial order m
F_{sat}^-	$f_s(k_r Z_r(1-s)/p - 2(1+k_a))$	$k_r Z_r - k_s Z_s - 2p(1+k_a)$
F_{sat}^0	$f_s(k_r Z_r(1-s)/p \pm 2k_a)$	$k_r Z_r - k_s Z_s \pm 2pk_a$
F_{sat}^+	$f_s(k_r Z_r(1-s)/p + 2(1+k_a))$	$k_r Z_r - k_s Z_s + 2p(1+k_a)$

As an example, for $Z_r = 38$, $Z_s = 48$ and $p = 2$ the highest saturation force harmonics are given by Table II. However, all the force harmonics of orders superior to 10 will create low magnitude vibrations, so the only important saturation force harmonic is F_{sat}^+ with order 2.

C. Experimental validation

An operational deflection shape (ODS) is run on a self-ventilated squirrel-cage induction machine with $Z_r = 38$, $Z_s = 48$ and $p = 2$ in order to visualize its stator vibrations. The visualised shape at frequency $f_s(Z_r(1-s)/p + 4)$ is

TABLE II
MAIN SATURATION FORCE LINES EXPRESSION OF TESTED MOTOR.

Name	Frequency f	Spatial order m
F_{sat}^-	$f_s(Z_r(1-s)/p - 4)$	-16
F_{sat}^0	$f_s(Z_r(1-s)/p - 2)$	-14
F_{sat}^+	$f_s(Z_r(1-s)/p + 2)$	-10
F_{sat}^+	$f_s(Z_r(1-s)/p + 4)$	-2

presented in Fig. 2. In agreement with Table II, an elliptical vibration is observed. This vibration resonates with the stator elliptical mode during starting phase when $f_s = f_2/(Z_r(1-s)/p + 4)$, where f_2 is the stator elliptical mode natural frequency.

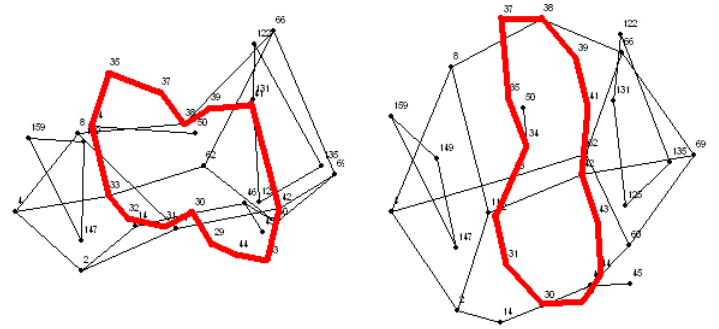


Fig. 2. Deflection shape of tested motor at $f_s(38/2 + 4) = 23f_s$, with $f_s = 30$ Hz (no load case), captured at two successive moments.

The effect of saturation level on noise has also been investigated by progressively increasing the air-gap flux ϕ_g at the fixed supply frequency where the saturation force wave excites stator elliptical mode. Results are displayed in Fig. 3.

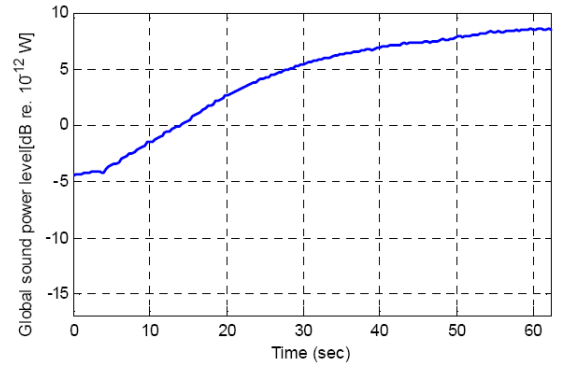


Fig. 3. Normalized evolution of sound power level due to saturation with time, when linearly increasing the air-gap flux from 2 to 7.5 V/Hz.

An empirical law has therefore been established to quantify the effect of saturation level on noise:

$$L_w \approx \alpha \log_{10}(\phi_g) + \beta \quad (8)$$

where α and β coefficients depend on the motor geometry, and iron magnetization curve (in tested motor, $\alpha = 22$). This law is useful for predicting how the maximum sound power level encountered during starting will be reduced using a lower air-gap flux.

D. Reduction of noise due to saturation

Z_r and Z_s are both involved in the expressions of saturation forces orders, their choice is therefore highly important to avoid saturation resonances. The great influence of slot combination as already been studied regarding magnetic noise due to slotting vibrations [24].

More precisely, the stator elliptical mode is the most dangerous one in traction motors, so one should avoid to excite this mode with high magnitude saturation vibrations during the whole starting phase (for $p = 2$, f_s typically goes from 0 to 100 Hz). In variable-speed applications, this is more easily done by avoiding to create any saturation force wave of order 2, than trying to avoid frequency match between saturation waves exciting frequencies and elliptical mode natural frequency.

Consequently, Z_r and Z_s should be chosen so that the largest saturation vibration (given by $k_a = k_r = k_s = 1$) has not a spatial order of 2, that is to say

$$|Z_r - Z_s \pm 2p, 4p| \neq 2 \quad (9)$$

Tested motor does not respect this rule as $|38 - 48 + 4 \times 2| = 2$. To respect this rule, a new rotor slot number can be chosen, for instance $Z_r = 36$. One can easily check that this new slot number satisfies equation (9). In the next part, some simulation and experiments are run in order to check if this new number of rotor slots decrease saturation noise.

III. SIMULATION RESULTS AND EXPERIMENTAL VALIDATION

A. Simulation results

Some simulation are run using a simulation tool called DIVA [18], which is able to determine the acoustic noise of magnetic source emitted by an induction machine, including load, pulse-width modulation (PWM) and saturation effects. This vibro-acoustic simulation software has been already validated on several motors [16], [25], [26], [27], [28] and at different stages by tests and finite element method (FEM). More details about the electrical model and vibro-acoustic models used in DIVA are given in those references, and especially how to compute the stator natural frequencies.

The magnitude of saturation permeance harmonics has been validated first with FEM software OPERA. The evolution of the saturated permeance harmonics magnitude with saturation was correct, but the analytical expression (6) did not give results accurate enough, so it has been necessary to introduce a proportional fitting coefficient (see Fig. 4).

The resulting radial flux density has been also validated with FEM (see Fig. 5).

The variable-speed noise radiated by both tested motor with $Z_r = 38$ and new proposed motor with $Z_r = 36$ has been simulated with DIVA (Fig. 6). The actual motor with $Z_r = 38$ has a strong resonance near $f_s = 30$ Hz, in agreement with both analytical predictions (cf. Table II) and experiments (cf. Fig. 2). The proposed motor does not have any strong magnetic resonance, and theoretically improves the noise level of 20 dB.

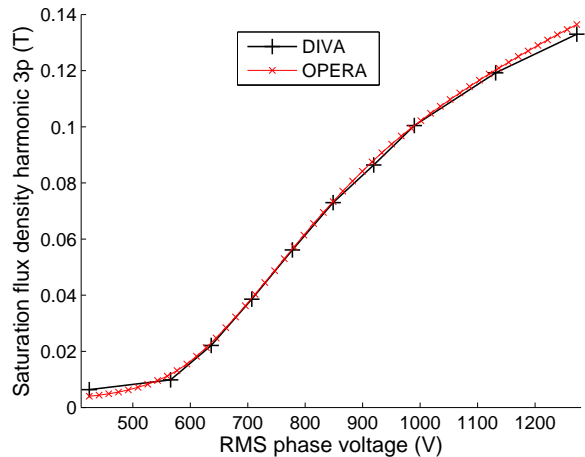


Fig. 4. FEM and DIVA main flux density saturation harmonic of spatial order $3p$ in function of the applied phase voltage, after having fit the analytical model.

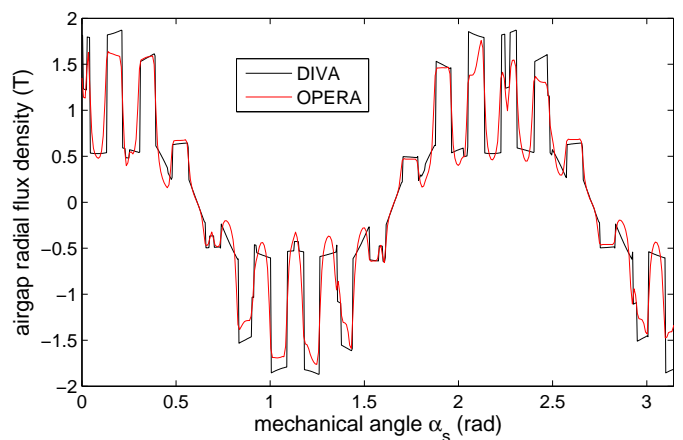


Fig. 5. FEM and DIVA flux density distribution along the air-gap in saturated case.

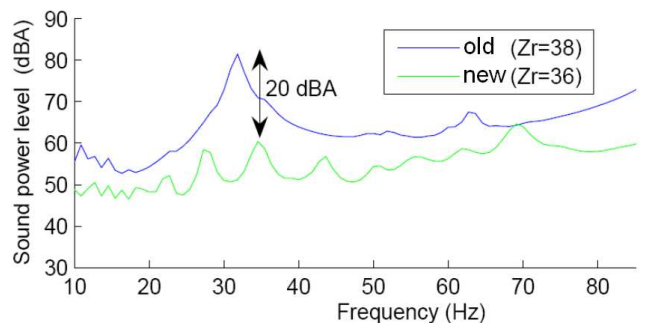


Fig. 6. Sound power level radiated by initial tested motor with $Z_r = 38$, where a strong saturation vibration resonates with stator elliptical mode, and by proposed motor with a 36 slots rotor.

B. Experimental results

Fig. 7 presents the noise measurements made on these two different rotors at variable-speed, in off-load sinusoidal case.

As predicted by DIVA model, the 38 slots rotor creates a strong resonance near 35 Hz, whereas no particular resonance is observed on the 36 rotor slots. The new motor noise level nearly evolves linearly with speed: it is now totally covered by

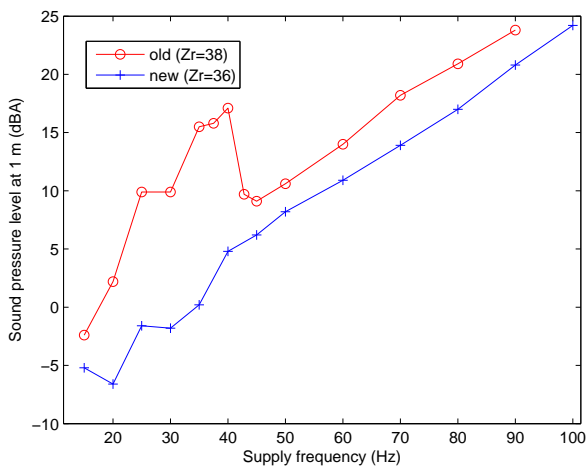


Fig. 7. Sound pressure level radiated by initial motor with $Z_r = 38$, where a strong saturation vibration resonates with stator elliptical mode, and by the proposed new motor with 36 rotor slots. A normalization factor has been introduced for confidentiality reasons.

fan noise. No noisy saturation vibration occurs, so that a larger saturation level can be used to higher starting torque without increasing magnetic noise level. Furthermore, a 15 dB on the overall noise (magnetic+aerodynamic) is obtained, against a predicted 20 dB on magnetic noise only.

IV. CONCLUSION

Magnetic noise due to saturation effects in induction machines has been analytically characterized, and these expressions have validated by experiments. They allow to predict possible resonances due to saturation, and a design rule has been proposed to avoid such resonances. This approach has been successfully validated with both simulation results, based on the analytical models, and experiments. A 15 dB decrease in sinusoidal case has been obtained by simply changing the number of rotor slots in order to avoid resonances due to Maxwell saturation forces.

REFERENCES

- [1] V. Lanfranchi, G. Friedrich, J. L. Besnerais, and M. Hecquet, "Spread spectrum strategies study for induction motor vibratory and acoustic behavior," in *Proceedings of the IECON*, Nov. 2006.
- [2] B. Cassoret, R. Corton, D. Roger, and J. Brudny, "Magnetic noise reduction of induction machines," *IEEE Trans. on Power Electronics*, vol. 18, no. 2, Mar. 2003.
- [3] R. Corton, B. Cassoret, and J. Brudny, "Characterization of three-phase harmonic systems generated by PWM inverter switching application to induction machine magnetic noise reduction," in *Proceedings of IEMDC*, 2001, pp. 442–447.
- [4] A. Hubert and G. Friedrich, "Influence of power converter on induction motor acoustic noise: interaction between control strategy and mechanical structure," *IEE Proc. on Electr. Power Appl.*, vol. 149, Mar. 2002.
- [5] K. Maliti and C. Sadarangani, "Modeling magnetic noise in induction machines," in *Proceedings of Electrical Machines and Drives Conference*, 1997, pp. 406–410.
- [6] A. Belahcen, "Vibrations of rotating electrical machines due to magneto-mechanical coupling and magnetostriction," *IEEE Trans. on Magnetics*, vol. 42, no. 4, Apr. 2006.
- [7] T. Hilgert, A. Vandeveld, and J. Melkebeek, "Numerical analysis of the contribution of magnetic forces and magnetostriction to the vibrations in induction machines," *IET Sci. Meas. Technol.*, vol. 1, no. 1, 2007.

- [8] P. Alger, *Induction machines : their behaviour and uses*. Gordon and Breach Science Publishers, 1970.
- [9] P. Timar, *Noise and vibration of electrical machines*. Elsevier, 1989.
- [10] H. Jordan, *Electric motor silencer - formation and elimination of the noises in the electric motors*. W. Giradet-Essen editor, 1950.
- [11] S. J. Yang, *Low noise electrical motors*. Oxford: Clarendon Press, 1981.
- [12] W. Soedel, *Vibrations of shells and plates*. Marcel Dekker, 1993.
- [13] S. Verma and A. Balan, "Determination of radial-forces in relation to noise and vibration problems of squirrel-cage induction motors," *IEEE Trans. on En. Conv.*, vol. 9, no. 2, June 1994.
- [14] G. Bossio, C. D. Angelo, J. Solsona, G. Garcia, and M. Valla, "A 2-D model of the induction machine: an extension of the modified winding function approach," *IEEE Trans. on Energy Conversion*, vol. 19, no. 1, Mar. 2004.
- [15] M. Poloujadoff, "General rotating mmf theory of squirrel cage induction machines with non-uniform air gap and several non sinusoidally distributed windings," *IEEE Trans. on P.A.S.*, vol. 101, no. 3, Mar. 1982.
- [16] J. L. Besnerais, V. Lanfranchi, M. Hecquet, P. Brochet, and G. Friedrich, "Acoustic noise of electromagnetic origin in a fractional-slot induction machine," *COMPEL*, vol. 27, no. 5, Feb. 2008.
- [17] W. Lo, C. Chan, Z. Zhu, L. Xu, D. Howe, and K. Chau, "Acoustic noise radiated by PWM-controlled induction machine drives," *IEEE Trans. on Industrial Electronics*, vol. 47, no. 4, Aug. 2000.
- [18] J. L. Besnerais, "Reduction of magnetic noise in PWM-supplied induction machines - low-noise design rules and multi-objective optimisation," Ph.D. dissertation, Ecole Centrale de Lille, France, Nov. 2008.
- [19] K. Maliti, "Modelling and analysis of magnetic noise in squirrel-cage induction motors," Ph.D. dissertation, Stockholm, 2000.
- [20] J. Moreira and T. Lipo, "Modeling of saturated AC machines including air gap flux harmonics components," *IEEE Trans. on Ind. Appl.*, vol. 28, 1992.
- [21] H. Frohne, "ber die primren bestimmungsgrößen der lautstärke bei asynchronmaschinen," Ph.D. dissertation, Hannover, Germany, 1959.
- [22] J. Brudny, "Modélisation de la denture des machines asynchrones : phénomènes de résonances," *Journal of Physics III*, vol. 37, no. 7, 1997.
- [23] H. D. Gersem, K. Hameyer, and T. Weiland, "Electromagnetically excited audible noise in electrical machines," *IEEE Trans. on Magnetics*, vol. 39, no. 3, May 2003.
- [24] T. Kobayashi, F. Tajima, M. Ito, and S. Shibukawa, "Effects of slot combination on acoustic noise from induction motors," *IEEE Trans. on Mag.*, vol. 33, no. 2, 1997.
- [25] J. L. Besnerais, V. Lanfranchi, M. Hecquet, and P. Brochet, "Multi-objective optimization of induction machines including mixed variables and noise minimization," *IEEE Trans. on Mag.*, vol. 44, no. 6, June 2008.
- [26] J. L. Besnerais, V. Lanfranchi, M. Hecquet, P. Brochet, and G. Friedrich, "Characterisation of the radial vibration force and vibration behaviour of a PWM-fed fractional-slot induction machine," *IET*, Nov. 2008.
- [27] J. L. Besnerais, V. Lanfranchi, M. Hecquet, and P. Brochet, "Characterization of the audible magnetic noise emitted by traction motors in railway rolling stock," in *Proc. of the INTERNOISE conference*, Shanghai, China, Oct. 2008.
- [28] J. L. Besnerais, A. Fasquelle, J. Pelle, S. Harmand, M. Hecquet, V. Lanfranchi, P. Brochet, and A. Randria, "Multiphysics modeling: electro-vibro-acoustics and heat transfer of induction machines," in *Proc. of the International Conference on Electrical Machines (ICEM'08)*, Villamura, Portugal, Sept. 2008.